



Self-ignition of polymerization fronts with convection: the 'rainstorm effect'

Simone Bidali¹, Arnaud Ducrot²*, Alberto Mariani¹*, Mauro Rustici¹

¹ Dipartimento di Chimica, Università di Sassari and INSTM local research unit, Via Vienna 2, 07100, Sassari, Italy; mariani@uniss.it

² UMR 5585 CNRS, Laboratoire de Mathématiques Appliquées, Ecole Centrale de Lyon, avenue Guy de Collongue, 69134 Ecully Cedex, France; Arnaud.Ducrot@ec-lyon.fr

(Received: January 29, 2005; published: June 30, 2005)

Abstract: This work is devoted to an experimental and numerical study on the influence of natural convection on the ignition of polymerization reaction fronts. Numerical simulations confirm experimental findings. Indeed, it has been observed that under the same initial and boundary conditions the front ignition can occur either in the centre of the reactor or at the top. The difference between these two cases is determined by the viscosity of the medium and by other parameters that can influence the convective motion of a liquid monomer. If the viscosity is low, weak convective motion in the beginning of the development of the reaction will lead to the accumulation of the hotter monomer at the top of the reactor. In this case, front ignition occurs at the top and propagates downwards (*rainstorm effect*). If the viscosity is sufficiently high, the convective motion does not essentially change the position of the emerging hot spot; the front appears at the centre of the reactor and propagates almost spherically outwards.

Introduction

Generally speaking, reaction ignition can be considered as a rapid jump of the reaction rate that goes from a negligible to a large value. If ignition takes place in the whole reactor, we speak of volumetric ignition, whereas, when it occurs in a localized domain, we speak of frontal ignition.

In combustion theory, the best-known phenomenon is the ignition of flames in a premixed gaseous mixture. The flame corresponds to the thin reaction zone, which separates the unburnt gas from the burnt one. The ignition process requires high activation energy and the reaction should be exothermic in order to have the possibility to propagate due to a diffusion process.

A similar process of ignition occurs in some reactions of macromolecular synthesis, generally named frontal polymerizations (FPs). FP is a method for the synthesis of macromolecules that exploits the heat released during an exothermic polymerization reaction. If the amount of dissipated heat is not excessive, a sufficient quantity of energy may induce the polymerization of the monomer in proximity of the hot zone. As a result, the formation of a hot polymerization front capable of self-sustaining and propagating throughout the whole reacting mixture is observed [1-21].

FP was initially studied in the former USSR: methyl methacrylate was polymerized under drastic pressure conditions (c. 3000 atm) [1,2]. Pojman *et al.* polymerized many other vinyl monomers at ambient pressure [3-8]. Besides, the curing of epoxy monomers has been performed frontally [9-13]. In recent years, Mariani *et al.* have widely investigated this field, mainly focusing on new chemical systems able to bring about FP, such as polyurethanes [14,15], unsaturated polyester resins [16,17], polydicyclopentadiene [18], and its interpenetrating polymer networks with polyacrylates [19]. Recently, frontal atom transfer radical polymerization [20] and frontal radical induced cationic polymerization [21] were also proposed.

In this work, we consider the influence of natural convection on the ignition of a polymerization front. This phenomenon can be particularly important from both an academic and a practical point of view. It can change the velocity of the front, its stability and form [22-27]. It is also well known that natural convection can influence the conditions of extinction of the front or change the ignition from frontal to volumetric. Furthermore, the occurrence of these phenomena is of great importance in handling and storage of reacting mixtures, also for safety reasons.

In the present paper, we compare our experimental results with a model proposed by us on the ignition process. It is shown that convection can change the critical values of parameters corresponding to ignition.

Experimental part

1,6-Diisocyanatohexane (HDI), 2-hydroxyethyl acrylate (HEA), *cis*-2-butene-1,4-diol (BD), Terathane[®] 1000 (TT, a polytetrahydrofuran with $M_n \approx 1000$), and dibutyltin dilaurate (DBTDL) were purchased from Aldrich. Pyrocatechol (PC) and benzoyl peroxide (BPO) were purchased from Fluka. Cab-O-Sil (fumed silica with a very large external surface area) was purchased from Riedel de Hahn. Aliquat[®] persulfate (APS, a liquid quaternary ammonium salt) was prepared as reported in ref. [28].

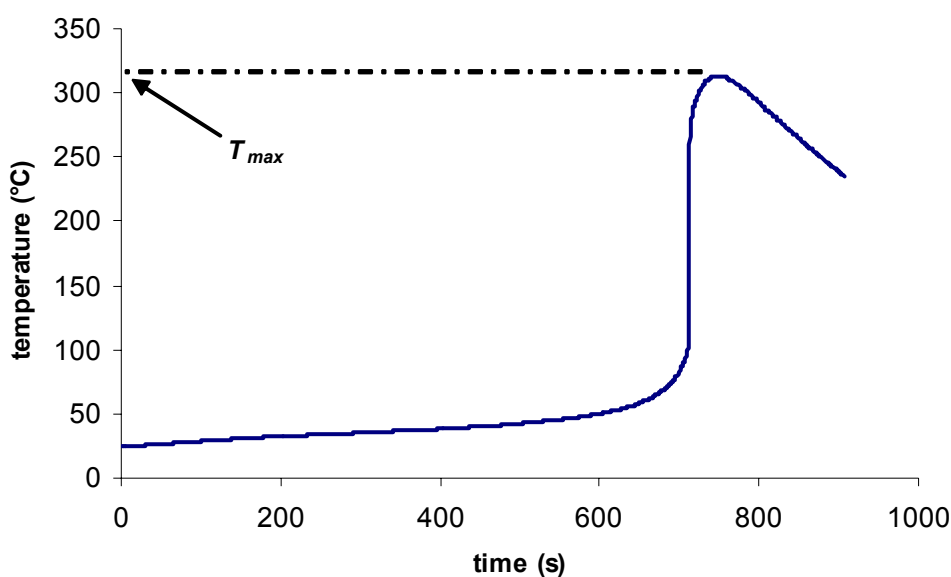


Fig. 1. Temperature profile recorded during a spontaneous FP (starting from the upper layer of the mixture) of a system B (see text) sample with 1.0 wt.-% Cab-O-Sil (sample 3B)

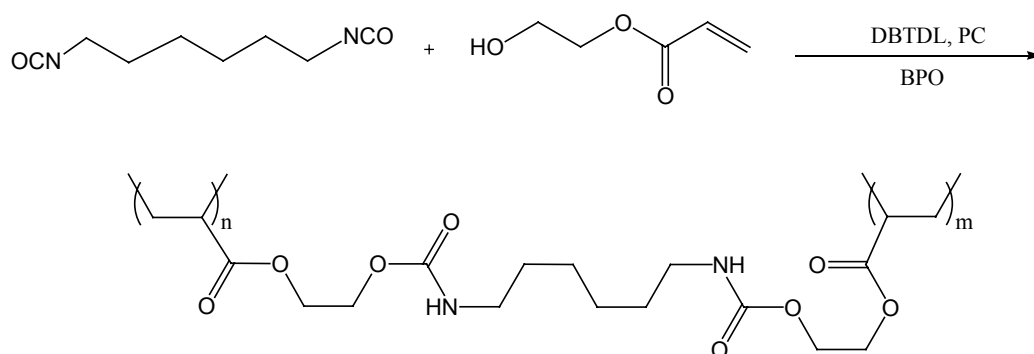
T_{in} indicates the initial temperature of the system. Pot life is measured from the time at which all reactants were mixed into the reaction tube until self-ignition. T_{max} is the maximum temperature reached by the polymerization front (Fig. 1).

As reactors, glass test tubes (inner diameter: 16 mm) were used. Reproducibility: T_{max} : $\pm 10^{\circ}\text{C}$; T_{in} : $\pm 0.1^{\circ}\text{C}$; pot life: ± 0.5 min.

All reactants were kept separately in a thermostated oil bath set at various T_{in} , rapidly added into a glass test tube and vigorously shaken therein. In order to minimize heat exchanges, all runs were conducted in 'adiabatic' reactors. The junctions of three thermocouples (joined to a digital recorder) were placed into the mixture at three different levels (1.0, 2.5 and 7.0 cm from the bottom of the tube, respectively).

Samples of system A were prepared by mixing, in a first vial, $1.00 \cdot 10^{-2}$ mol of BD, $5.00 \cdot 10^{-3}$ mol of TT, $1.50 \cdot 10^{-6}$ mol of DBTDL (catalyst for the formation of urethane groups). In a second vial, $1.50 \cdot 10^{-2}$ mol of HDI, $1.65 \cdot 10^{-4}$ mol of PC (inhibitor of the above catalyst) and $3.77 \cdot 10^{-4}$ mol of APS (radical initiator for the polymerization of double bonds) were added. These vials were placed in a thermostated oil bath at the desired temperature (T_{in}) until thermal equilibrium. Afterwards, the two contents were rapidly poured into the same glass test tube. Immediately after, 2.5 wt.-% of Cab-O-Sil were added and the mixture was vigorously shaken.

Similarly, samples of system B (Scheme 1) were prepared by pouring into a glass test tube the contents of two vials previously thermally equilibrated at the requested temperature: in the first, $7.54 \cdot 10^{-6}$ mol of DBTDL were added to $7.54 \cdot 10^{-2}$ mol of HEA; in the second, $3.77 \cdot 10^{-2}$ mol of HDI, $7.54 \cdot 10^{-4}$ mol of PC, and $3.77 \cdot 10^{-4}$ mol of BPO (radical initiator) were mixed. To some samples of system B, Cab-O-Sil was added (1B, 2B, 3B and 5B).



Scheme 1. Polymer network formation in system B

Results and discussion

Experimental study

During our studies on the binary FP for the formation of IPNs (interpenetrating polymer networks) constituted of polyacrylates and polyurethanes, we have unexpectedly observed an intriguing phenomenon, which occurs under certain conditions. Indeed, several polymerizing mixtures kept at room temperature undergo spontaneous ignition in a localized zone thus resulting in a FP. Furthermore, depending on the reaction parameters, such an ignition has been noticed to take place in the upper layer or in the geometrical centre of the reacting mixture (Fig. 2).

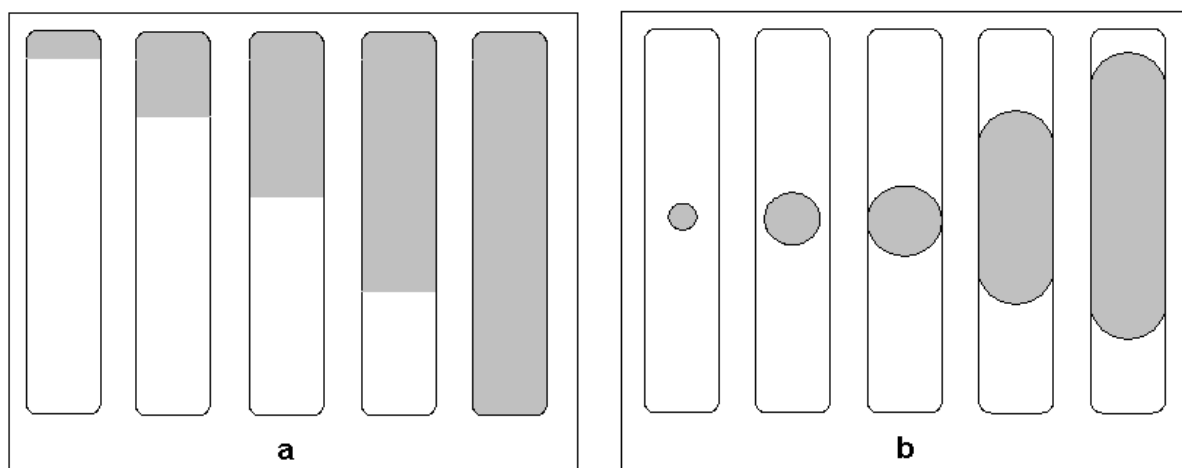


Fig. 2. Schematic representations of FP (unreacted mixture: white; polymer: grey). a) Typical descending front propagation (ignition is in the upper layer of the reacting mixture); b) 'spherical' front propagating from the centre of the mixture

In particular, the self-formation of two polymer networks, obtained by the reaction of system A and B, respectively, was studied. We underline here that both reacting mixtures were characterized by the simultaneous presence of vinyl groups, which polymerize by a free-radical mechanism, and isocyanate and hydroxyl groups to form urethanes. Some of those groups are present on the same molecule. Furthermore, we have found that, in the systems studied in the present work, all components reported in the Experimental part are necessary in order to observe this phenomenon.

Selected data of spontaneous polymerizations underwent by system A, in which a relatively large amount of Cab-O-Sil is present (2.5 wt.-%), are reported in Tab. 1. In these experiments, the role of Cab-O-Sil is that of increasing medium viscosity and thus avoiding fingering formation [29]. As expected, the higher T_{in} , the shorter the pot life, this latter being dramatically influenced also by small variations of the initial temperature. At variance, T_{max} does not seem to be dependent on T_{in} . In all reported runs, spontaneous FP happened starting from the top of the mixture.

Tab. 1. Data of selected runs of system A in which spontaneous FP occurred (2.5 wt.-% Cab-O-Sil)

Sample	T_{in} in °C	Pot life in min	T_{max} in °C	Self-ignition position
1A	20	40	89	top
2A	23	35	72	top
3A	24	35	100	top
4A	25	35	88	top
5A	28	17	101	top
6A	33	9.0	106	top

However, after these preliminary experiments, we turned our attention to system B because it was found to be less complicated; in fact, (i) only one reactant bears hydroxyl groups; (ii) fingering was not observed even when Cab-O-Sil was not

present; moreover, (iii) the mutual solubility among its components is larger than those of system A. For this reason, all data discussed hereafter deal with system B.

Tab. 2 refers to runs conducted in the presence of the same quantity of Cab-O-Sil (1.0 wt.-%). As expected, in this case too it can be noted that the higher T_{in} , the shorter the pot life. However, at variance to system A, T_{max} increases monotonically as T_{in} rises. When T_{in} is set at 27°C (corresponding to a mixture with relatively low viscosity), ignition takes place at the top of the mixture instead of at its geometrical centre. This finding suggests that also small differences of initial temperature (2°C) are sufficient to create a viscosity variation able to change the position in which ignition takes place.

Tab. 2. Runs performed on system B starting from various T_{in} (1.0 wt.-% Cab-O-Sil)

Sample	T_{in} in °C	Pot life in min	T_{max} in °C	Self-ignition position
1B	20	17	290	centre
2B	25	16	296	centre
3B	27	12	315	top

Tab. 3. Experiments performed on system B as a function of the amount of viscosifier ($T_{in} = 25^\circ\text{C}$)

Sample	Cab-O-Sil (wt.-%)	Pot life in min	T_{max} in °C	Self-ignition position
4B	0.0	13	292	top
2B	1.0	16	296	centre
5B	2.0	46	304	centre

In Tab. 3, data related to the variation of the quantity of viscosifier are listed (in all these runs, $T_{in} = 25^\circ\text{C}$). As displayed, the higher the Cab-O-Sil content, the longer the pot life. Namely, the variation of viscosity, resulting from the addition of 2.0 wt.-% Cab-O-Sil, extended pot life dramatically from 13 - 16 to 46 min.

Moreover, a significantly different behaviour was observed even when only 1.0 wt.-% Cab-O-Sil was added. Indeed, at variance to what was found when no viscosifier was present, the position from which FP spontaneously started was not the top, but the geometrical centre of the reaction mixture (Fig. 2).

By summarizing the above observations: such reactive systems have a pot life in the order of tens of minutes; during this period the reaction mixtures start to polymerize with heat release; this generates convective motion in variable extents depending on the medium viscosity. In particular, when the latter is relatively low (*i.e.*, T_{in} is relatively high and/or no viscosifier is present, or it is present in little amount), convective motions cause the accumulation of hot materials in the upper layers of the reaction mixture and of cold materials in the lower part of the reactor. When a 'critical' temperature (roughly around 60°C) is reached, the self-ignition occurs from the top of the mixture. The result is a spontaneous FP, which rapidly propagates downwards (Fig. 2a). For the similarity to some meteorological event, we propose the name *rainstorm effect* for this phenomenon.

In contrast, when medium viscosity is relatively high (*i.e.*, T_{in} is low and/or a significant amount of viscosifier is present) the hottest zone is the geometrical centre of the reaction mixture, being characterized by the minimum amount of heat loss due to thermal exchange through the tube walls. In this case, spontaneous FP is observed which propagates in a ‘spherical’ fashion towards all directions (Fig. 2). As also evidenced in this figure, apart from reactor geometry, fronts generated from the centre are not really spherical; indeed, due to convection, upwards propagation is faster than that downwards. A similar behaviour was already found by Asakura *et al.* [30].

In Fig. 3, the temperature profiles simultaneously recorded by the three thermocouples (see Experimental part) are reported for a run in which ignition took place at the centre. Indeed, the temperature jump is firstly recorded by the central thermocouple (curve b) and then by the other two, placed over and under the first one.

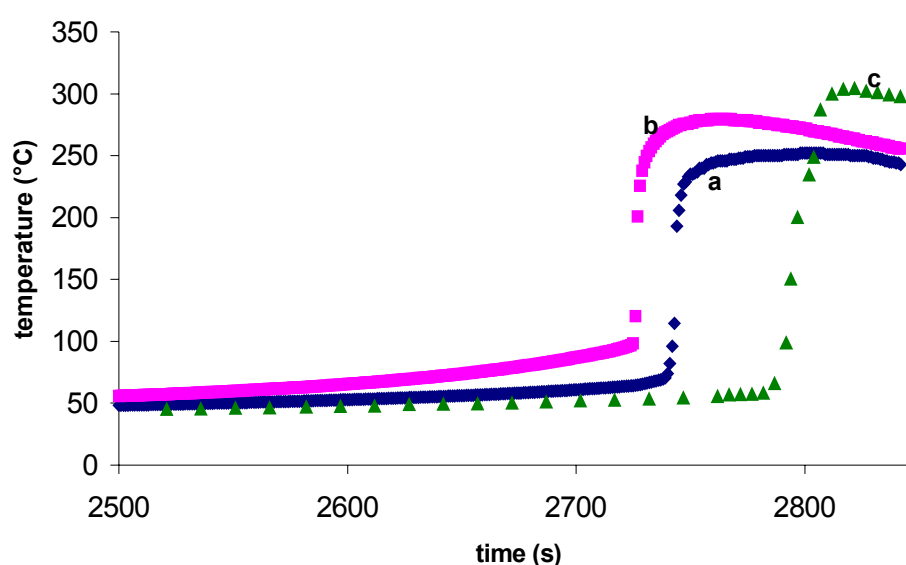


Fig. 3. Spontaneous FP profiles acquired during the phenomenon of self-ignition starting from the geometrical centre of the reacting mixture. Curves a, b and c are referred to data recorded at 1.0, 2.5 and 7.0 cm from the bottom of the tube, respectively (sample 2B)

Tab. 4. Data related to some experiments conducted on system B without Cab-O-Sil starting from various T_{in}

Sample	T_{in} in °C	Pot life in min	T_{max} in °C	$T_{max} - T_{in}$	Self-ignition position
6B	15	42	291	276	top
1B	20	17	285	265	top
4B	25	13	292	267	top
7B	30	10	298	268	top
8B	35	8.0	315	280	top
9B	40	7.0	342	302	top
10B	45	5.5	312	267	top
11B	50	4.0	321	271	top

We have also studied the effect of T_{in} on the behaviour of system B in the absence of Cab-O-Sil. Initial temperature was allowed to vary from 15 to 50°C (Tab. 4). This range has been chosen because, at lower T , pot lives become very long (in the order of many hours), whereas at temperatures that are higher than 50°C, pot lives are too short. Actually, as can be seen also by temperature profiles, self-ignition always occurred at about 55 - 65°C. Data reported in Tab. 4 clearly indicate that pot life dramatically decreased when T_{in} changed from 15°C (pot life = 42 min) to 20°C (pot life = 17 min), and much less rapidly at higher temperature.

In all cases, the rainstorm effect was observed with a spontaneous and sudden ignition of FP from the upper layer of the reacting mixture and a fast front propagation downwards. Moreover, except for sample 9B ($T_{max} - T_{in} = 302^\circ\text{C}$), the difference between T_{max} and T_{in} is confined in a range of 15°C (265°C for 1B and 280°C for 8B): this indicates that the 'degree of adiabacity' was practically the same in any experiment.

Modelling of the problem

This part is devoted to a numerical study of ignition with convection. We consider a complete model taking into account the depletion of reactants. In order to study qualitative properties, we suppose that the chemical reaction corresponding to the polymerization process is simple and of order one.

In this model we do not take into account the possible complex kinetics of the polymerization process. This simplification is currently used when studying ignition of the reaction front. Indeed, it is well known that simple chemistry describes well front propagation in combustion theory [31]. In addition, there are some examples of polymerization kinetics described by first order reactions, like radical polymerization discussed in ref. [32] (see also the references therein).

Complete model with consumption

In this section we present a mathematical model describing the evolution of the temperature and of the concentration of reactants. The system consists of the reaction-diffusion equations coupled with the Navier-Stokes equations under the Boussinesq approximation:

$$\frac{\partial \theta}{\partial t} + u \frac{\partial \theta}{\partial x} + v \frac{\partial \theta}{\partial y} = \Delta \theta + f(\theta)Y \quad (1)$$

$$\frac{\partial Y}{\partial t} + u \frac{\partial Y}{\partial x} + v \frac{\partial Y}{\partial y} = \Lambda \Delta Y - f(\theta)Y \quad (2)$$

$$\frac{\partial u}{\partial t} + u \frac{\partial u}{\partial x} + v \frac{\partial u}{\partial y} = P \Delta u - \frac{\partial p}{\partial x} \quad (3)$$

$$\frac{\partial v}{\partial t} + u \frac{\partial v}{\partial x} + v \frac{\partial v}{\partial y} = P \Delta v - \frac{\partial p}{\partial y} + R\theta \quad (4)$$

$$\frac{\partial u}{\partial x} + \frac{\partial v}{\partial y} = 0 \quad (5)$$

Here θ is the dimensionless temperature, Y the reactant concentration, $\mathbf{V} = (u, v)$ the velocity of the medium, p the pressure. The non-dimensional parameters are the inverse of the Lewis number Λ , the Prandtl number P , and the Rayleigh number R .

The term $f(\theta)$ describes the temperature dependence of the reaction rate. It is usually taken in the form of the Arrhenius exponential. Here, we approximate it by the usual exponential

$$f(\theta) = Z^2 e^{Z(\theta - 1)}$$

where the parameter Z is the Zeldovich number.

The system (1) - (5) is considered in a two-dimensional rectangular domain

$$D = (0, L_x) \times (0, L_y)$$

and is supplemented with some boundary and initial conditions.

More precisely, we consider the Robin boundary condition for the temperature

$$\frac{\partial \theta}{\partial n} = -\sigma \theta \quad (6)$$

where σ is a non-negative parameter. The homogeneous Neumann boundary condition for the concentration and free surface boundary conditions for the velocity are

$$\frac{\partial Y}{\partial n} = 0 \quad (7)$$

$$x = 0, L_x u = 0, \frac{\partial v}{\partial x} = 0, y = 0, L_y v = 0, \frac{\partial u}{\partial x} = 0 \quad (8)$$

The initial conditions are:

$$\theta(0, x, y) = 0, Y(0, x, y) = 1, u(0, x, y) = v(0, x, y) = 0 \text{ for } (x, y) \in D \quad (9)$$

In order to study the problem (1) - (9), we use the stream function-vorticity formulation. The stream function ψ is defined by

$$u = \frac{\partial \psi}{\partial x}, v = -\frac{\partial \psi}{\partial y}$$

and $\psi = 0$ on ∂D , while the vorticity ω is

$$\omega = -\Delta \psi$$

Note that, thanks to Eq. (8), the function ω satisfies $\omega = 0$ on ∂D .

With these variables, system (1) - (5) re-writes:

$$\frac{\partial \theta}{\partial t} + u \frac{\partial \theta}{\partial x} + v \frac{\partial \theta}{\partial y} = \Delta \theta + f(\theta) Y \quad (10)$$

$$\frac{\partial Y}{\partial t} + u \frac{\partial Y}{\partial x} + v \frac{\partial Y}{\partial y} = \Lambda \Delta Y - f(\theta) Y \quad (11)$$

$$\frac{\partial \omega}{\partial t} + u \frac{\partial \omega}{\partial x} + v \frac{\partial \omega}{\partial y} = P \Delta \omega - PR \frac{\partial \theta}{\partial x} \quad (12)$$

$$\Delta \psi + \omega = 0 \quad (13)$$

The system is supplemented with the boundary conditions:

$$\frac{\partial \theta}{\partial n} = -\sigma \theta$$

$$\frac{\partial Y}{\partial n} = 0$$

$$\psi = \omega = 0 \text{ on } \partial D$$

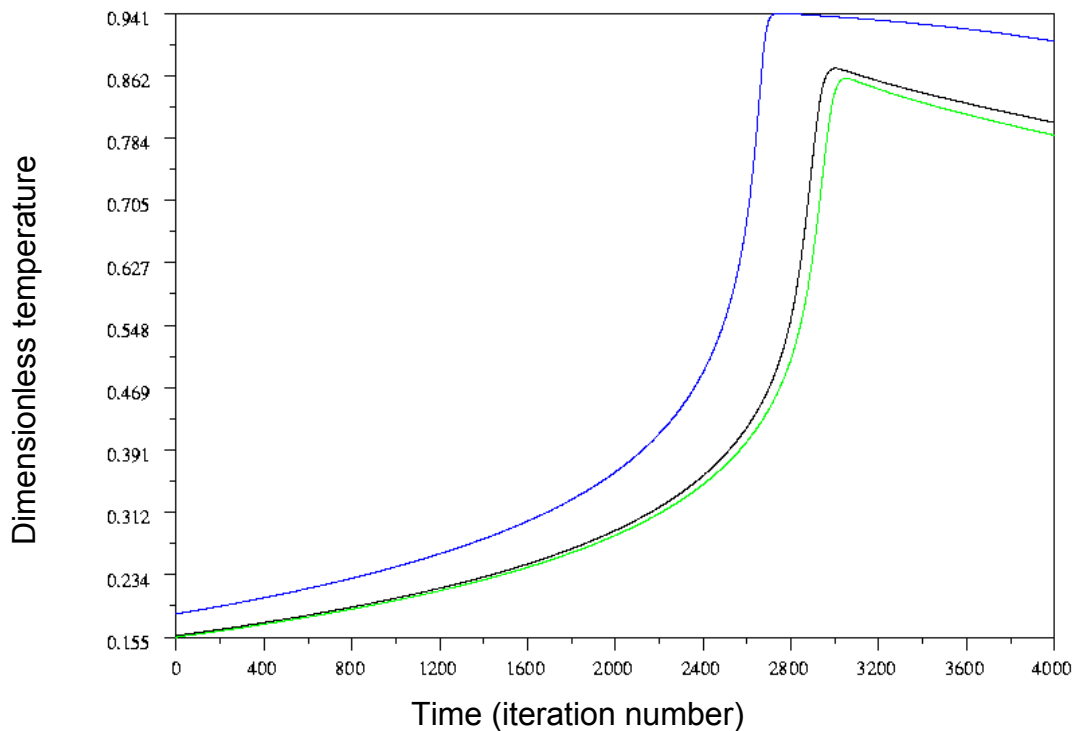
and the initial conditions

$$\theta(0, x, y) = 0, \quad Y(0, x, y) = 1, \quad \psi(0, x, y) = \omega(0, x, y) = 0 \text{ for } (x, y) \in D$$

We use a finite difference approximation and an alternating direction method to solve the system (10) - (13) together with the corresponding boundary conditions.

Numerical results

In this section we present numerical simulations corresponding to different values of the Rayleigh number, which is inversely proportional to the viscosity of the fluid. The numerical simulations were conducted with a fixed Prandtl number $P = 3$, a fixed Zeldovich number $Z = 9.5$, $L_x = L_y = 8$ and finally $\Lambda = 1$. We also give some results for $\Lambda = 0.5$.



----- Temperature at the top - - - - - Temperature in the middle - - - - - Temperature at the bottom

Fig. 4. Evolution of the temperature for $Z = 9.5$, $R = 5$ and $\Lambda = 1$

For sufficiently small Rayleigh numbers, the front has the same behaviour as in the case without convection (corresponding to $R = 0$). It starts at the centre of the bulk

and propagates spherically. Convection is weak and there are two vortices symmetric with respect to the centreline (see Figs. 4 - 6). In Fig. 4, we also see that the temperatures at the bottom and at the top are very close, while the temperature at the centre is always higher than that near the reactor walls.

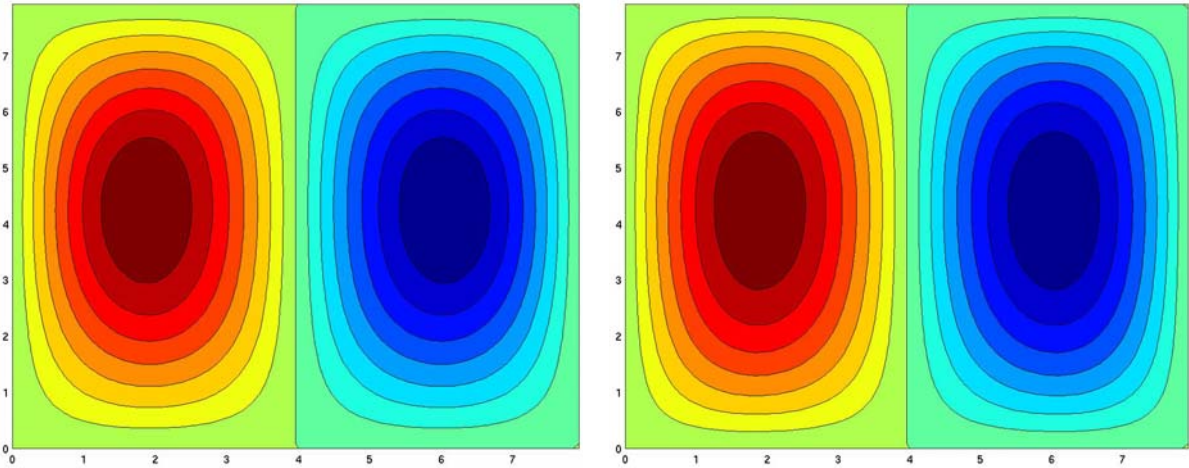


Fig. 5. Level lines of the stream function at consecutive moments of time for $R = 5$

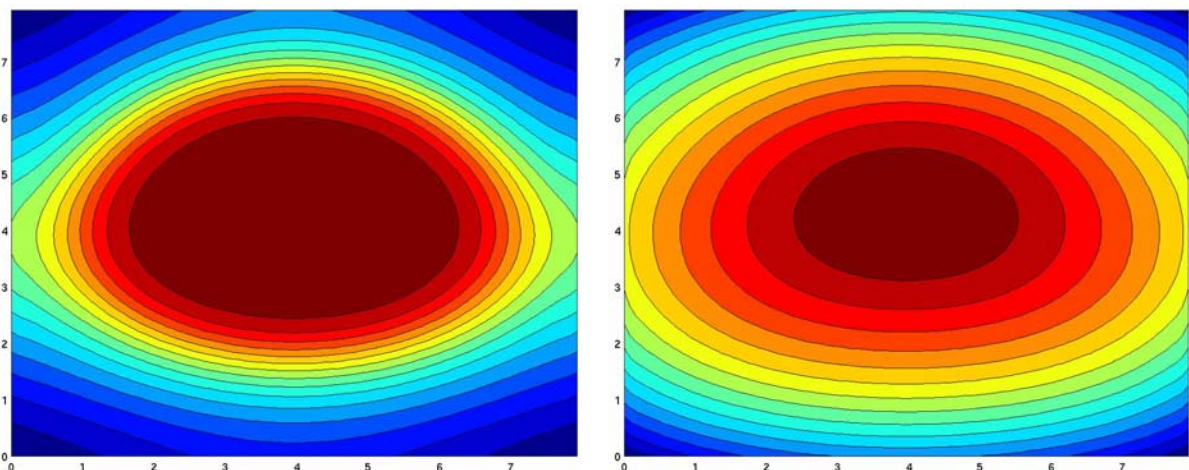
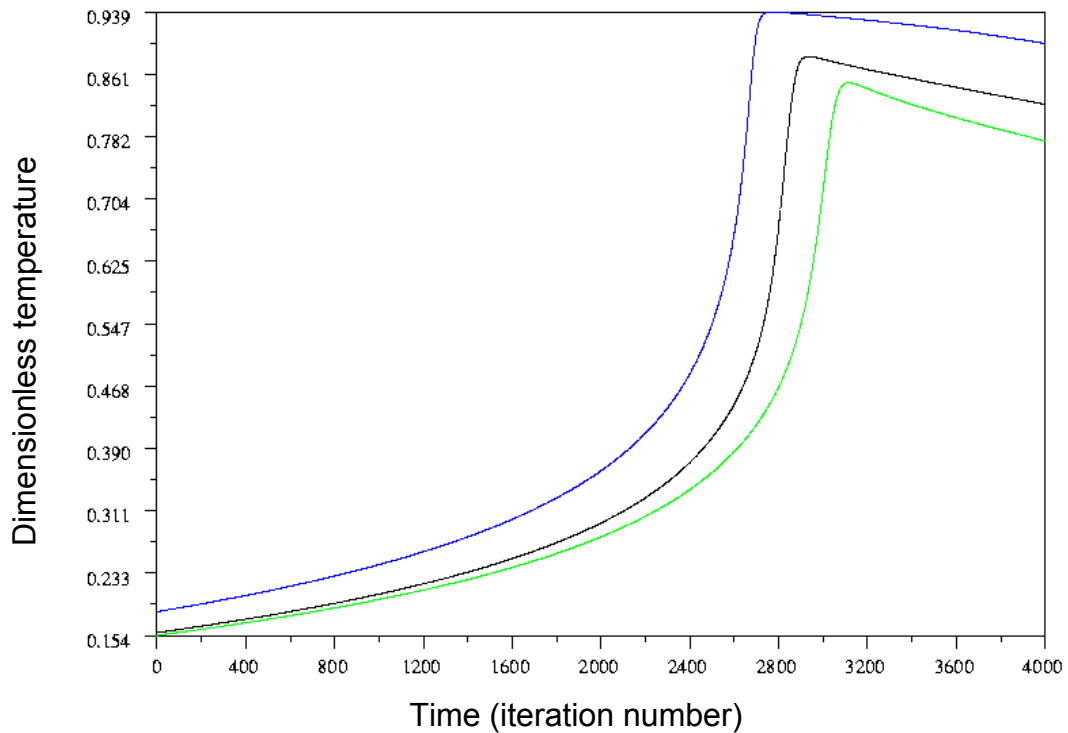


Fig. 6. Isotherms at consecutive moments of time for $R = 5$

When the parameter R is increased, the ignition of the reaction front occurs higher in the reactor. For $R = 20$, we first observe that the temperatures at bottom and top are not close anymore (Fig. 7). The temperature at the top is higher than that at the bottom. It is the first effect of the convection, which brings hot liquid to the top of the reactor.

The convection is weak enough, and the hot spot remains near the centre of the bulk. Indeed, we can see that the temperature at the centre is always higher than that at the boundary.

In addition, Fig. 9 shows that the hot spot appears higher in the bulk than in the previous case with $R = 5$ (Fig. 6). We also see that the shape of the front becomes elliptic. The isostreams are represented by a symmetric two-vortex mode (see Fig. 8).



----- Temperature at the top - - - - - Temperature in the middle - - - - - Temperature at the bottom

Fig. 7. Evolution of the temperature for $Z = 9.5$, $R = 20$ and $\Lambda = 1$

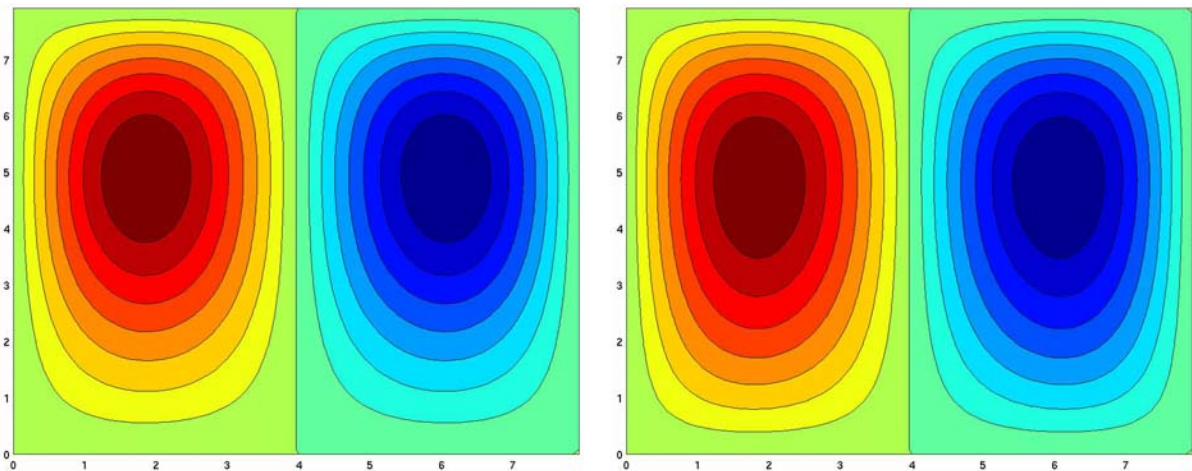


Fig. 8. Level lines of the stream function at consecutive moments of time for $R = 20$

For $R = 1000$, the temperature at the top of the reactor becomes maximal, the temperature at the centre is lower but close to it, while the temperature at the bottom is essentially lower (Fig. 10). This means that the front starts at the top of the reactor and propagates rapidly downwards along the preheated monomer. When it passes the centre of the reactor, the speed of propagation decreases because there the temperature of the monomer is lower.

It is interesting to note that behind the front the temperature at the centre becomes higher than the temperature at the top, then lower, and finally again higher (Fig. 10). It can be related to the influence of heat loss through the walls of the reactor and of the convective motion. The isotherms in Fig. 10 show that the front is rather flat being

more advanced from the sides due to convection. The interaction of the convective motion with the reaction front changes also the form of the vortices, which are more compressed in the centre of the reactor (Fig. 9). For $R = 5000$, in Fig. 13 it is shown that the ignition occurs at the top of the reactor.

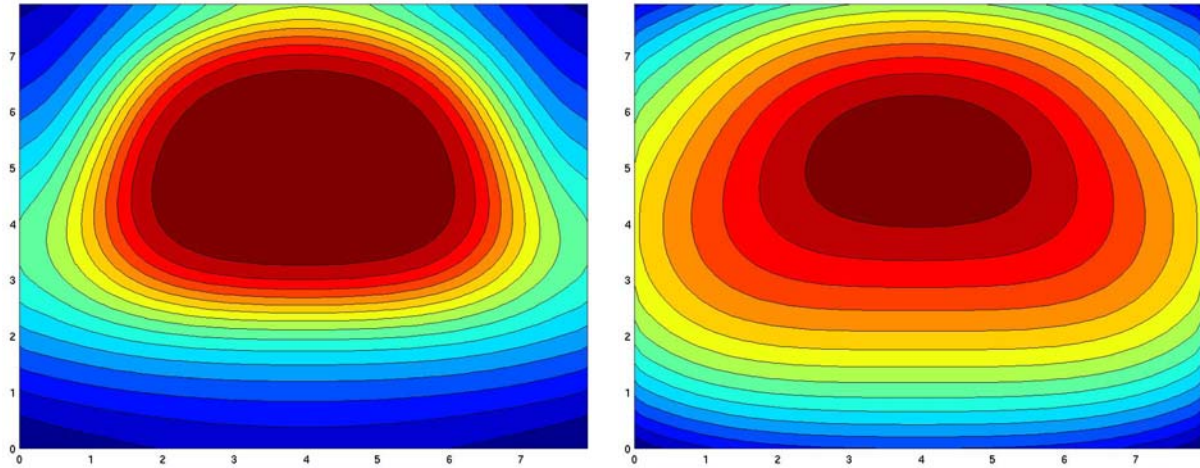
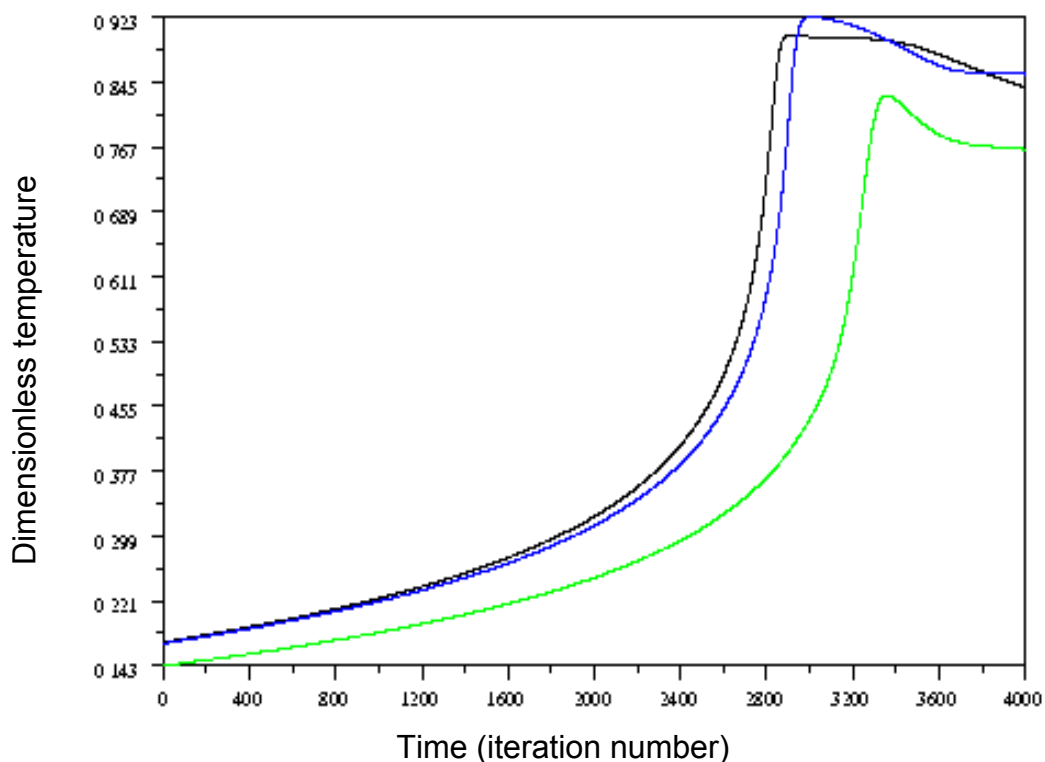


Fig. 9. Isotherms at consecutive moments of time for $R = 20$



----- Temperature at the top - - - - - Temperature in the middle - - - - - Temperature at the bottom

Fig. 10. Evolution of the temperature for $Z = 9.5$, $R = 1000$ and $\Lambda = 1$

After the ignition, the corresponding curve is strongly non-monotone. This phenomenon corresponds to the interaction of the heat loss at the top and the convection that brings hot liquid from the bottom. There are four vortices instead of the two observed for lower values of the Rayleigh number.

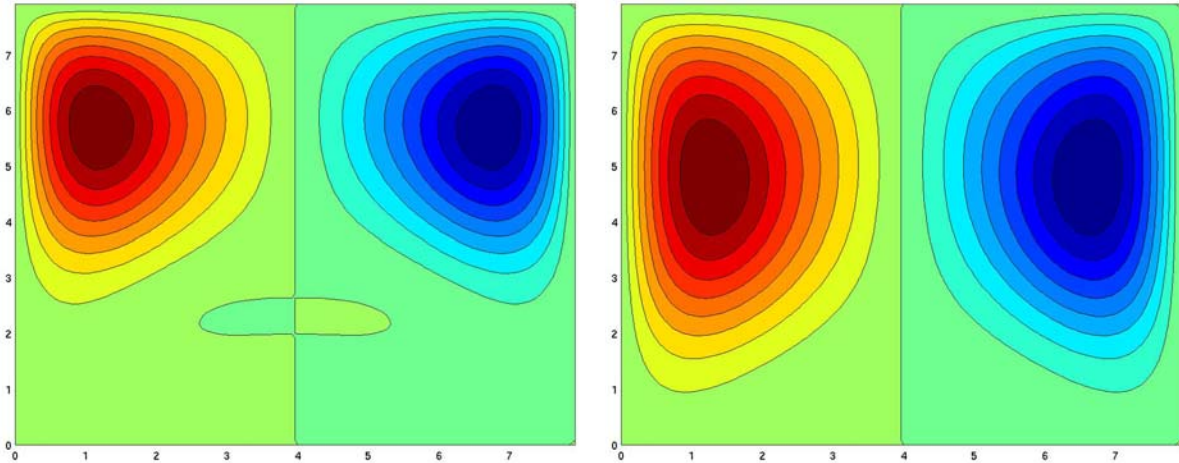


Fig. 11. Level lines of stream function at consecutive moments of time for $R = 1000$

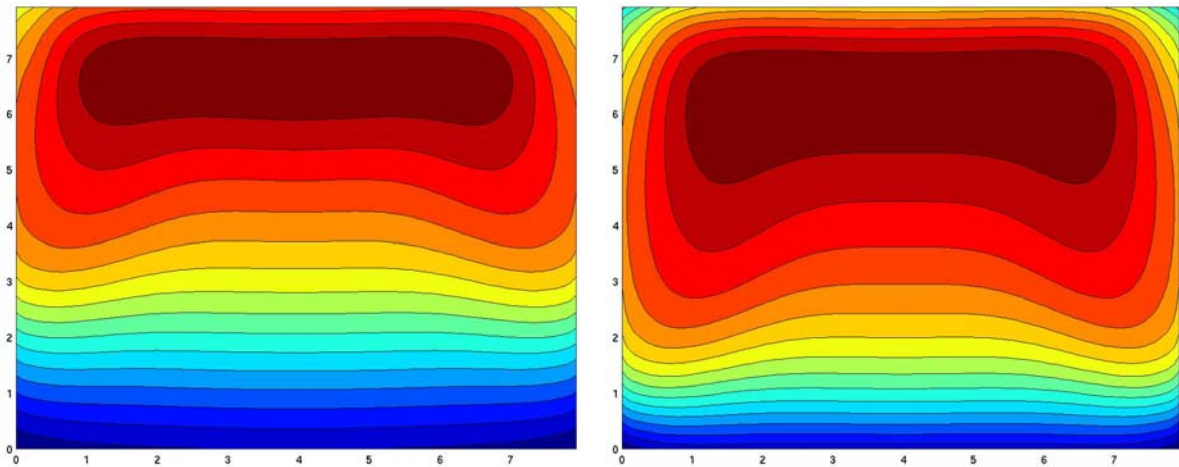
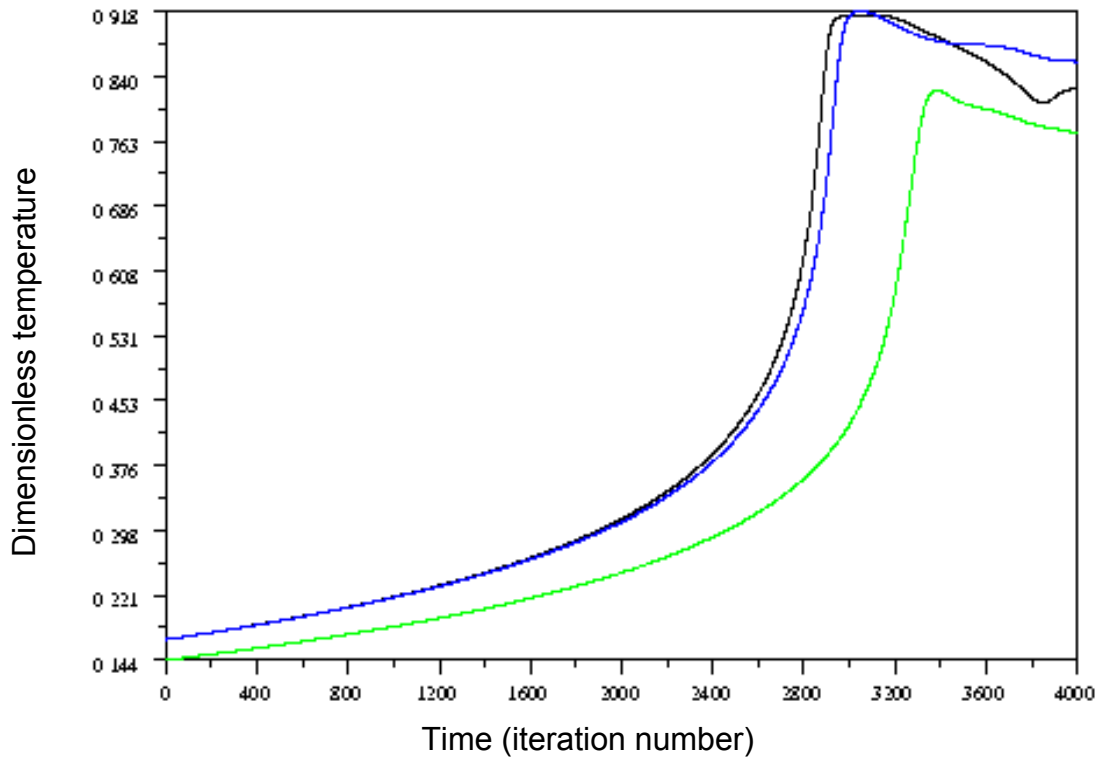


Fig. 12. Isotherms at consecutive moments of time for $R = 1000$

Finally, in Fig. 15 we see that a hot spot develops and the front starts to propagate. It is initially flat but convection is strong enough to change its form. It tends to become more curved on its upper part, that corresponds to a decrease of the temperature at the top. Finally the hot spot splits into two hot spots symmetric with respect to the centre line. Similar results can be obtained for different values of the Lewis number.

We present here an example of ignition followed by front propagation for $\Lambda = 0.5$. In Fig. 16, we show the evolution of the temperature at the centreline at different moments of time. The above curves correspond to the early stage of the reaction while the upper ones correspond to the end of the reaction. Note that the time step between two curves used in Fig. 16 is not the same for those corresponding to pre-heating of the mixture and for the ignition. Indeed, these two phenomena have not the same characteristic times.

In Fig. 16, we can see that the temperature starts to rise uniformly in the bulk. After some time, it becomes quite lower at the boundary due to the heat loss. Due to the strongly non-linear effect of the reaction rate, this difference between the temperature at the centre and that at the boundary increases. As a consequence, we observe the development of the reaction front at the centre. The result is a front that propagates spherically outwards.



----- Temperature at the top -.-.-.- Temperature in the middle -.-.-.- Temperature at the bottom

Fig. 13. Evolution of the temperature for $Z = 9.5$, $R = 5000$ and $\Lambda = 1$

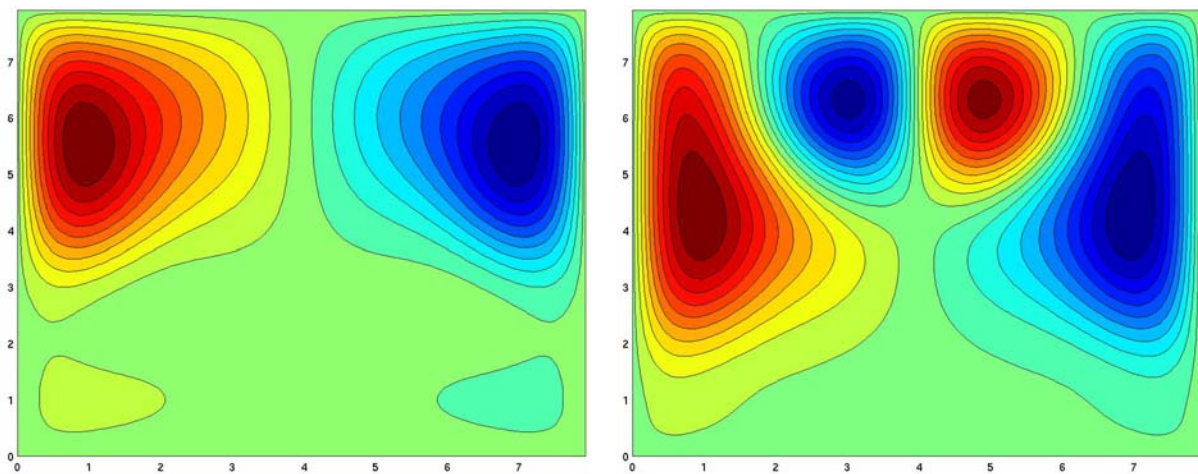


Fig. 14. Level lines of the stream function at consecutive moments of time for $R = 5000$

We change next the boundary condition for the temperature. Here the flux is proportional to the difference $\theta - \theta_0$, where θ_0 is the temperature of the bath

$$\frac{\partial \theta}{\partial n} = -\sigma(\theta - \theta_0)$$

We see that the parameter θ_0 allows us to influence the ignition process. With a small Rayleigh number, increasing the temperature θ_0 allows to obtain a reaction front that starts at the top of the reactor.

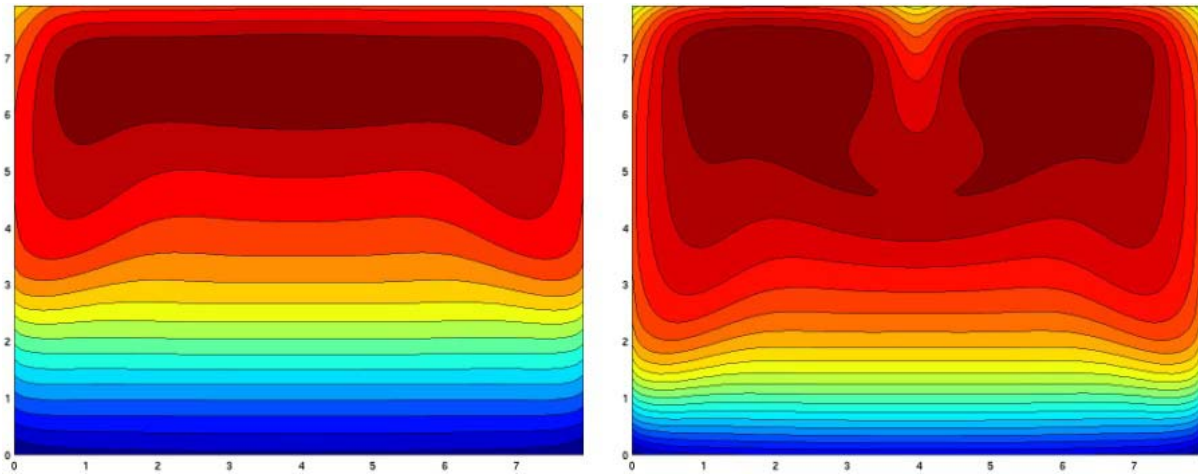


Fig. 15. Isotherms at consecutive moments of time for $R = 5000$

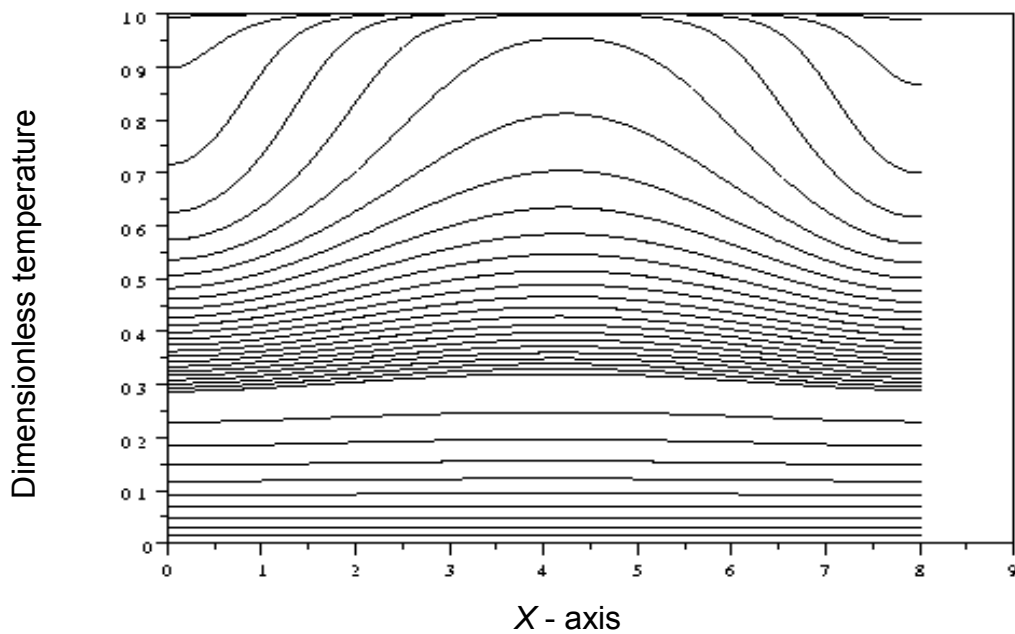


Fig. 16. Ignition and propagation of the reaction front for $R = 5$ and $\Lambda = 0.5$

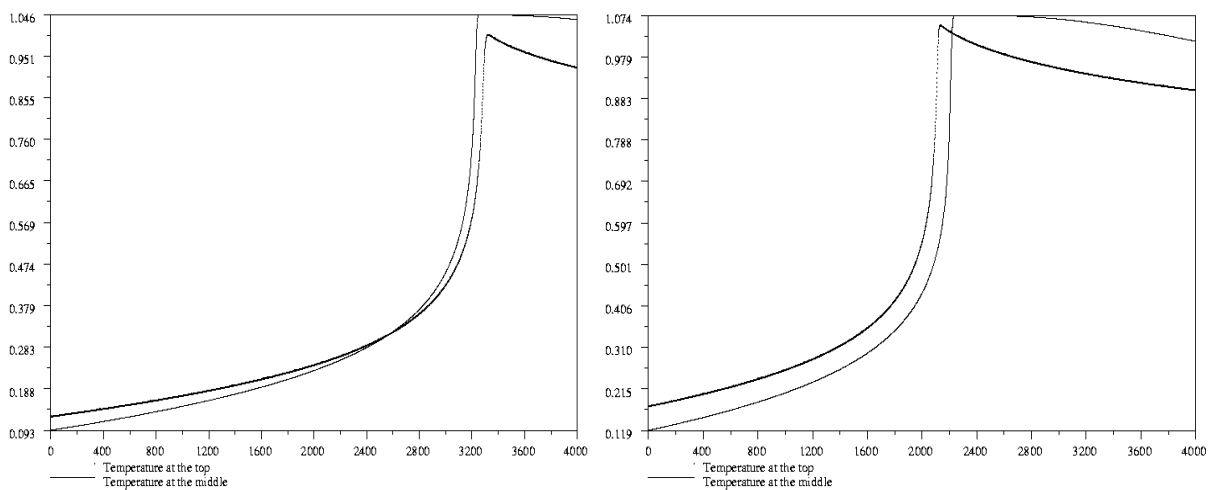


Fig. 17. Sensibility to the parameter θ_0 for $R = 20$. Evolution of the temperature for $\theta_0 = 0.2$ (left) and $\theta_0 = 0.3$ (right)

For $R = 20$, according to the above results, the ignition of the front starts at the centre for $\theta_0 = 0$. For $\theta_0 = 0.2$, we see that the same holds true, at variance to the case $\theta_0 = 0.3$, for which the ignition front starts at the top (see Fig. 17). This parameter decreases the ignition time of the reaction (see Fig. 18).

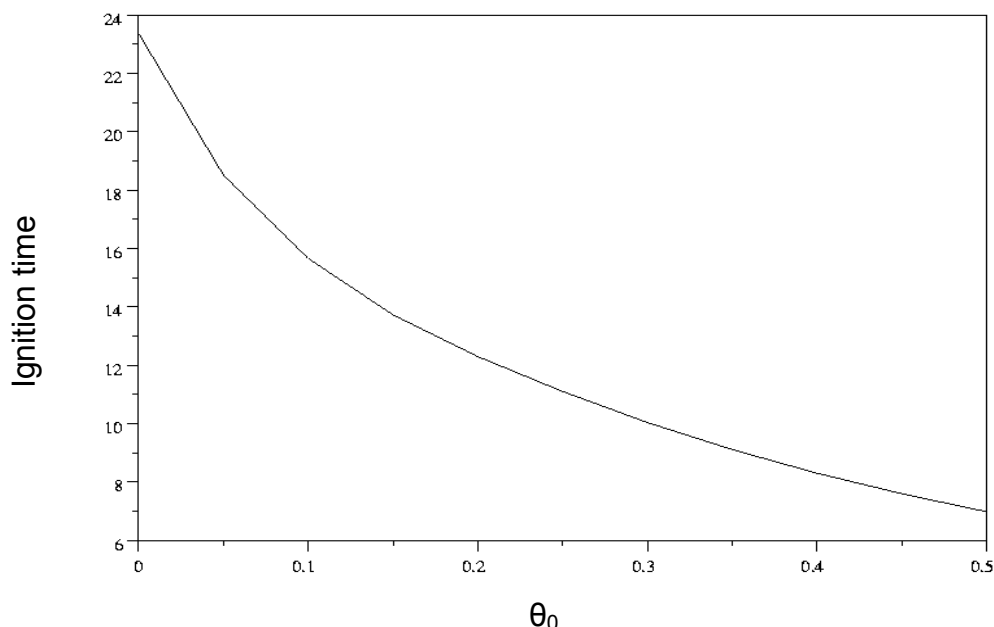


Fig. 18. Ignition time as a function of θ_0

Conclusions

To conclude, we can say that the numerical simulations confirm the main phenomena experimentally found. Indeed, we have experimentally observed that when viscosity is increased by Cab-O-Sil (or, in a less dramatic way, by decreasing temperature), the self-ignition of frontal polymerization changes place. This result is completely confirmed by the numerical simulation corresponding to different values of the Rayleigh number, which is an inverse function of kinematic viscosity. The simulation shows that in the absence of convection (high viscosity, low Rayleigh number) self-ignition starts at the centre of the bulk, while in the presence of convection (low viscosity, high Rayleigh number) self-ignition starts at the top of the reacting mixture.

We have also observed that the temperature of the bath can change the ignition time. More particularly, the latter decreases when the external temperature increases, which is also something related to a critical viscosity variation. In addition, raising the oil bath temperature increases the heat exchange with the exterior medium. As a result, convection becomes stronger and brings up the preheated liquid to the top of the reactor, where the ignition front can start (rainstorm effect).

The model does not take into account the density dependence on the depth of conversion. However, at the initial stage of the reaction, where the depth of conversion is low, this effect can be neglected.

Acknowledgement: INSTM funds are gratefully acknowledged.

- [1] Chechilo, N. M.; Enikolopyan, N. S.; *Dokl. Phys. Chem.* **1975**, 221, 392.
- [2] Chechilo, N. M.; Enikolopyan, N. S.; *Dokl. Phys. Chem.* **1976**, 230, 840.
- [3] Pojman, J. A.; *J. Am. Chem. Soc.* **1991**, 113, 6284.
- [4] Khan, A. M.; Pojman, J. A.; *Trends Polym. Sci.* **1996**, 4, 253.
- [5] Fortenberry, D. I.; Pojman, J. A.; *J. Polym. Sci., Part A: Polym. Chem.* **2000**, 38, 1129.
- [6] Bazile, M., Jr.; Nichols, A.; Pojman, J. A.; Volpert, V.; *J. Polym. Sci., Part A: Polym. Chem.* **2002**, 40, 3504.
- [7] Pojman, J. A.; Varisli, B.; Perryman, A.; Edwards, C.; Hoyle, C.; *Macromolecules* **2004**, 37, 691.
- [8] McFarland, B.; Popwell, S.; Pojman, J. A.; *Macromolecules* **2004**, 37, 6670.
- [9] Chekanov, Y.; Arrington, D.; Brust, G.; Pojman, J. A.; *J. Appl. Polym. Sci.* **1997**, 66, 1209.
- [10] Kim, C.; Teng, H.; Tucker, C. L., III; White, S. R.; *J. Comp. Mater.* **1995**, 29, 1222.
- [11] Pojman, J. A.; Elcan, W.; Khan, A. M.; Mathias, L.; *J. Polym. Sci., Part A: Polym. Chem.* **1997**, 35, 227.
- [12] Gill, N.; Pojman, J. A.; Willis, J.; Whitehead, J. B., Jr.; *J. Polym. Sci., Part A: Polym. Chem.* **2003**, 41, 204.
- [13] Mc Farland, B.; Popwell, S.; Pojman, J. A.; *Macromolecules* **2004**, 37, 6670.
- [14] Fiori, S.; Mariani, A.; Ricco, L.; Russo, S.; *Macromolecules* **2003**, 36, 2674.
- [15] Mariani, A.; Bidali, S.; Fiori, S.; Malucelli, G.; Sanna, E.; *e-Polymers* **2003**, no. 044.
- [16] Bidali, S.; Fiori, S.; Malucelli, G.; Mariani, A.; *e-Polymers* **2004**, no. 001.
- [17] Fiori, S.; Malucelli, G.; Mariani, A.; Ricco, L.; Russo, S.; *e-Polymers* **2002**, no. 057.
- [18] Mariani, A.; Fiori, S.; Chekanov, Y.; Pojman, J. A.; *Macromolecules* **2001**, 34, 6539.
- [19] Fiori, S.; Mariani, A.; Ricco, L.; Russo, S.; *e-Polymers* **2002**, no. 029.
- [20] Fiori, S.; Mariani, A.; Bidali, S.; Malucelli, G.; *e-Polymers* **2003**, no. 060.
- [21] Mariani, A.; Bidali, S.; Fiori, S.; Sangermano, M.; Malucelli, G.; Bongiovanni, R.; Priola, A.; *J. Polym. Sci., Part A: Polym. Chem.* **2003**, 41, 204.
- [22] Golubev, V. B.; Gromov, K. G.; Guseva, L. R.; Korolev, B. A.; Kostarev, K. G.; Lyubimova, T. P.; *Heat Transfer Research* **1993**, 25, 888.
- [23] Briskman, V. A.; Kostarev, K. G.; Lyubimova, T. P.; Levto, V. L.; Mashinsky, A. L.; Nechitailo, G. S.; Romanov, V. V.; *Acta Astronautica* **1996**, 39, 395.
- [24] Mc Caughney, B.; Pojman, J. A.; Simmons, C.; Volpert, V. A.; *Chaos* **1998**, 8, 520.
- [25] Garbey, M.; Taik, A.; Volpert, V.; *Quart. Appl. Math.* **1998**, 53, 1.
- [26] Bowden, G.; Garbey, M.; Ilyashenko, V.; Pojman, J. A.; Solovyov, S.; Volpert, V. J.; *Chem. Phys. B* **1997**, 101, 678.
- [27] Garbey, M.; Taik, A.; Volpert, V.; *Quart. Appl. Math.* **1996**, 54, 225.

- [28] Masere, J.; Chekanov, Y.; Warren, J. R.; Stewart, F.; Al-Kaysi, R.; Rasmussen, J. K.; Pojman, J. A.; *J. Polym. Sci., Part A: Polym. Chem.* **2000**, *38*, 3984.
- [29] Pojman, J. A.; Craven, R.; Khan, A.; West, W.; *J. Phys. Chem.* **1992**, *96*, 7466.
- [30] Asakara, K.; Nihei, E.; Harasawa, H.; Ikumo, A.; Osanai, S.; in “*Nonlinear Dynamics in Polymeric Systems*”, ACS Symp. Ser. **2003**, *869*, Pojman, J. A.; Tran-Cong-Miyata, Q.; editors; American Chemical Society, p. 135.
- [31] Zeldovich, Y. B.; Barenblatt, G. I.; Librovich, V. B.; Makhviladze, G. M.; in “*The Mathematical Theory of Combustion and Explosions*”, Plenum, New York **1985**.
- [32] Pojman, J. A.; Volpert, V. A.; Volpert, V. I. A.; in “*Self-Propagating High-Temperature Synthesis of Materials*”, Borisov, A. A.; De Luca, L. T.; Merzhanov, A. G.; editors; Taylor and Francis, New York **2002**, 99.